Journal of Colloid and Interface Science 354 (2011) 139–143

Contents lists available at ScienceDirect

Journal of Colloid and Interface Science

www.elsevier.com/locate/jcis

Preparation of magnetic polymer particles with nanoparticles of Fe(0)

S. Buendía [a], G. Cabañas [b], G. Álvarez-Lucio [c], H. Montiel-Sánchez [d], M.E. Navarro-Clemente [a], M. Corea [a,*]

[a] Instituto Politécnico Nacional, ESIQIE, Edificio Z-6, Del. Gustavo A. Madero, C.P. 07738, Col. San Pedro Zacatenco, México DF, Mexico
[b] Instituto Politécnico Nacional, ESFM, UPALM, Edificio 9, Del. Gustavo A Madero, C.P. 07738, Col San Pedro Zacatenco, México DF, Mexico
[c] Universidad Nacional Autónoma de México, IIM, Circuito Exterior S/N C.P. 04510, Cd. Universitaria, Adpo. Postal 70-360, México DF, Mexico
[d] Universidad Nacional Autónoma de México, CCADET, Circuito Exterior S/N C.P. 04510, Cd. Universitaria, Adpo. Postal 70-186, México DF, Mexico

ARTICLE INFO

Article history:
Received 11 August 2010
Accepted 24 September 2010
Available online 14 October 2010

Keywords:
Magnetic polymers
Iron particles
Nanocomposites
Magnetic properties

ABSTRACT

Iron nanoparticles (Fe(0)), were encapsulated into polymethyl methacrylate (PMMA), by means of emulsion polymerization techniques in a semicontinuous process. The final average diameter of the composite particle was calculated until three times of average particle of iron particles and were stabilized with a non-ionic surfactant. They were then characterized by scanning electron microscopy and dynamic light scattering. Their magnetic properties were determined by parallel field vibrating-sample magnetometry method. The results indicated that the magnetic properties are a function of polymer concentration in the nanocomposite particle.

1. Introduction

"Nanotechnology" refers to materials on the nanometer scale, typically ranging in size from 100 nm down to the atomic. These materials differ from other materials due to following two principal factors: increased surface area and quantum effects [1]. Due to their unique electronic, optical magnetic and catalytic properties compared with the corresponding bulk material and molecules, the number of potential applications of these particles is growing rapidly [2,3].

However, metal nanoparticles typically agglomerate due to a highly active surface area. To stabilize and control the nanoparticles structure various surfactants, polymers, dendrimers, biological templates and biomacromolecules have been used [4,5].

Encapsulation of inorganic nanoparticles into polymers endows particles with important properties that bare particles lack, including an improved dispersibility and chemical stability and reduced toxicity, in addition to preventing the agglomeration of the inorganic particles [6–9].

Conventional methods for introducing inorganic nanoparticles into polymers can be divided into [10,11]: (1) coating the magnetic nanoparticles directly with the polymer, such as emulsion–solvent evaporation [12]; (2) filling the magnetic nanoparticles into porous presynthesized polymer particles form example swelling [13]; (3) dispersing the magnetic nanoparticles during the synthesis of polymer particles such as suspension, dispersion, emulsion and mini/micro-emulsion polymerization in the presence of metal nanoparticles [8,14,15]; and (4) the encapsulation of oil in water magnetic droplets as a seed for emulsion polymerization process with a hydrophobic monomer [16,17].

In more recent years, many novel applications of magnetic polymers have been proposed and researched in the fields as environmental and biomolecular bioseparations, in magnetic resonance imaging (as contrast agents), in magnetic drug targeting [18] and delivery [19–21] and as a potential cancer therapies (through hyperthermia) [22–24]. These materials exhibit a fast and very strong response to external magnetic fields. The application of even a modest external magnetic field results in a strong magnetic interaction leading to aggregation in complex networks [25,26]. Magnetic nanocomposites are found to have zero remanence. When a magnetic field is applied, a small dipole moment is induced in the particles; however, this moment disappears once the field is removed [27].

A magnetic material can be defined as a material that interacts with a magnetic field, and this interaction can be either attractive toward a magnetic pole (ferro- and paramagnetism) or repulsive (diamagnetism).

The application of a magnetic field (H) results in magnetization (M) of a sample [28]. When a ferromagnetic material is magnetized by increasing applied field and the field decrease; the magnetization does not follow the initial magnetization curve obtained during the increase. This irreversibility is called hysteresis [29]. In a typical hysteresis loop the response of the material follows two distinct paths upon magnetization and demagnetization. In large fields, magnetization approaches the maximum value or saturation magnetization (M_S). Coercivity (H_C) characterizes the reverse field

* Corresponding author. Fax: +52 5557296000.
E-mail addresses: mnavarroc@ipn.mx (M.E. Navarro-Clemente), mcorea@ipn.mx, mcoreat@yahoo.com.mx (M. Corea).

0021-9797/$ - see front matter © 2010 Elsevier Inc. All rights reserved.
doi:10.1016/j.jcis.2010.09.076

strength needed to reduce the magnetization to zero. Thus, hysteresis measurements provide obtaining information about coercivity, remnant magnetization, and saturation of a given material [30–32].

In this work, iron particles were chosen for encapsulation due to their high initial susceptibility and saturation magnetization [33–35]. Iron (Fe^0) particles with a average diameter of particle of 66 nm determinated by dynamic light scattering, were encapsulated into polymethyl methacrylate by means of emulsion polymerization techniques in a semicontinuous process. The polymerization reaction was made in presence of a surfactant because this kind of material has a tendency to aggregate, showing poor dispersion behavior when introduced into various polymer matrices [36]. The number of iron particles was kept constant in the system. The final average diameter of the composite particle was calculated until three times of average particle of iron particles. The resulting of magnetic properties measurement by parallel field vibrating-sample magnetometry of the encapsulated particles were found to be a function of polymer content in the particles.

2. Experimental

2.1. Materials

In order to synthesis of iron particles the reactives used were: the hexamethyldisilazane $HN[Si(CH_3)_3]_2$ the iron bromine (II) ($FeBr_2$) and n-Butyl lithium (C_4H_9Li) (from Aldrich). They were grade reactive and were used as received. The THF, diethyl ether and pentane (from Aldrich), were distilled, and degassed by means of methods knows and stored in an anaerobic chamber [37]. The Bis[bis(trimethylsilyl)amido]iron(II) $[Fe[N(Si(CH_3)_3)_2]_2]$ precursor of iron particles was used as it was obtained.

In order to encapsulation of iron particles the monomers used, methyl methacrylate (MMA) and potassium persulfate (from Aldrich) were grade reactive. The monomer was distilled and degassed. Rhodasurf L-4 (Rhodia) was employed as a surfactant no ionic. The surfactant and potassium persulfate were used as received. The dispersion medium was distilled and degassed water.

2.2. Synthesis of iron nanoparticles

The reactions were carried out on batch experiments. The Bis[bis(trimethylsilyl)amido]iron(II) $[Fe[N(Si(CH_3)_3)_2]_2]$ was obtained by the following reaction [38]:

$$FeBr_2(THF)_2 + 2LiN[Si(CH_3)_3]_2 \xrightarrow{Et_2O} Fe[N(Si(CH_3)_3)_2]_2 + 2LiBr + 2THF$$

0.1297 g (0.345 mmol) of $Fe[N(Si(CH_3)_3)_2]_2$ was dissolved in pentane. The solution was put in a pressure reactor. The reactor was pressurized at 3 bar of H_2 and the reaction was carried out at room temperature. The iron nanoparticles were produced by the following reaction:

$$Fe\left[N(SiMe_3)_2\right]_2 + H_2 \xrightarrow{pentene} Fe^0 + 2HN(SiMe_3)_2$$

The time of reaction was 12 h, after this, a black precipitate was obtained. The particles formed were translated to Schlenk flask, dried with vacuum; and were stored in sealed vials to prevent oxidation.

2.3. Encapsulation of nanoparticles

The nanocomposites were prepared via emulsion polymerization. Reactions were carried out in a semicontinuous reactor consisting of a jacketed rector and a feeding tank. The iron particles were used as seed particles. A continuous flow of pre-emulsion material was ensured by a dosing pump. The reactor consisted of a 250 mL stirred glass reactor under a dynamic flow of N_2 and at a temperature of 70 °C, controlled by a thermal bath. The concentration of the surfactant was maintained below the critical micellar concentration (CMC) in the pre-emulsion to ensure the absence of micelles [8,39]. The stirring rate was adjusted to 250 rpm. The formulation used to prepare the nanocomposites with once, twice and three times the final average diameter of Fe^0 particle are presented in Table 1.

2.4. Scanning electron microscopy (SEM) and X-ray energy dispersive (EDX) microanalysis

The average diameter and the distribution of particles sizes of iron nanoparticles were determined using SEM by the software called GATAM included in the software of microscope. The sample was sputtered with gold and placed in a scanning electronic microscope FEI model Sirion and measured at 5 kV.

The presence of Fe^0 and oxygen into the iron particles was determined by means of X-ray energy dispersive at 15 kV.

2.5. Dynamic light scattering (DLS)

The hydrodynamic diameter of iron nanoparticles, encapsulated with PMMA was determined using dynamic light scattering (DLS). The sample was measured at 25 °C, using a Malvern Zetasizer Nano ZS instrument. The particle size distribution was calculated using the software provided by Malvern with the equipment.

2.6. Magnetization measurement

The magnetic properties of the bare iron nanaoparticles and the encapsulated nanoparticles were measured by means of vibrating-sample magnetometry using LDJ model 9600. The samples were placed in a capillary tube, in an inert atmosphere of nitrogen and sealed. The maximum magnetic field applied was 10 Oe.

3. Results and discussion

The iron particles used were synthesized in a previous work, from The Bis[bis(trimethylsilyl)amido]iron(II) was decomposed under controlled conditions yields $HN(SiMe_3)_2$ and iron by treating iron powder. The iron powder was treating with hydrogen (H_2) under pressure for produced iron particles (Fe^0).

From the SEM analyses and measurements of dynamic light scattering, different particle diameter moments (number average diameter D_n; weight average diameter D_w), were calculated using the Eqs. (1) and (2), and the polydispersity index (PDI) was determined using Eq. (3) [40,41]:

$$D_n = \frac{\sum n_i D_i}{\sum n_i} \quad (1)$$

$$D_W = \frac{\sum n_i D_i^4}{\sum n_i D_i^3} \quad (2)$$

$$PDI = \frac{D_W}{D_n} \quad (3)$$

where n_i is the number of nanocomposites particles with diameter D_i.

The SEM image in Fig. 1, shows the purified particles of Fe^0, which exhibited spherical morphology and low polydispersity. The Fe^0 particles size distribution obtained using SEM and DLS are compared in Fig. 1a and b: the average diameters of these dried

Table 1
Polymerization recipes for once (recipe 1), twice (recipe 2) and three times (recipe 3) final average diameter of Fe^0 particle.

Reactive	Reactor (g)	Addition tank		
		Recipe 1	Recipe 2	Recipe 3
Fe^0 particles	0.02			
MMA		1.26	2.52	3.78
$Na_2S_2O_8$	6e−4	0.1007	0.2014	0.301
Rhodasurf L-4 (Rhodia) 0.004 wt.%	0.26	4.09	8.18	12.27
Water	16.0	41.66	83.34	125.01

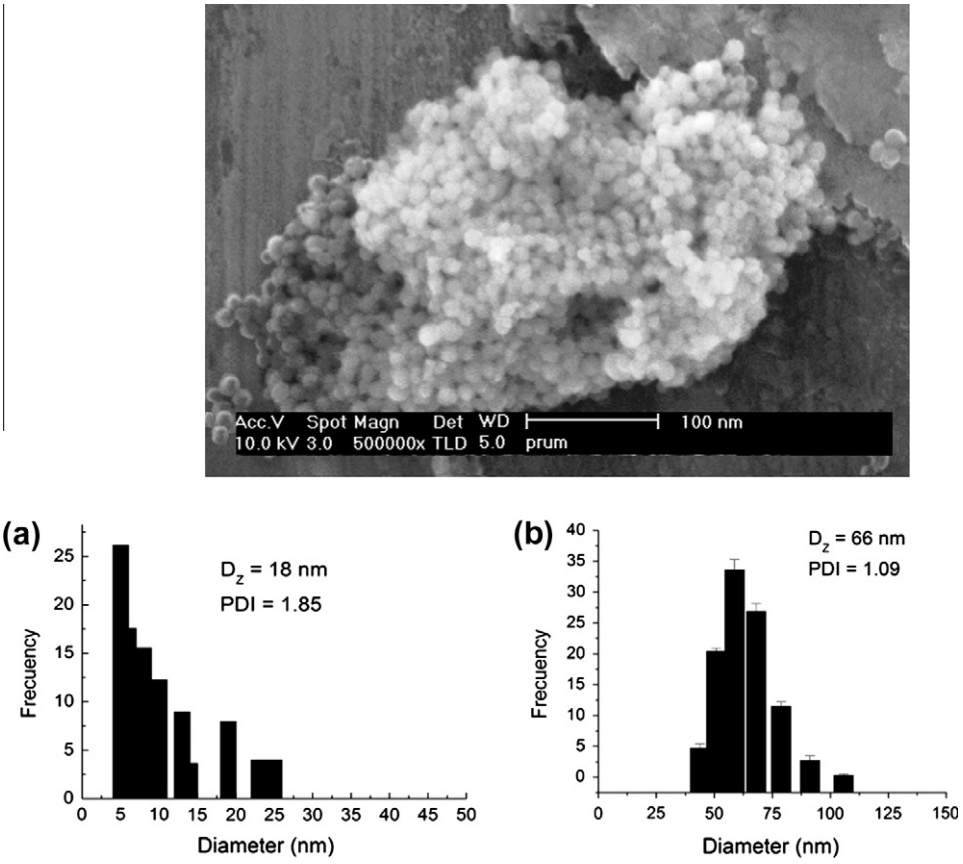

Fig. 1. Scanning electronic images of Fe^0 particles and the average particle diameter distribution of particle determined by: (a) SEM and (b) dynamic light scattering.

microspheres were determined by the two techniques to be 18 nm and 66 nm respectively.

The EDX spectrum for the Fe^0 particles is shown in Fig. 2. The K_α, K_β, L_α and $L_{\beta 1}$ lines, characteristics of Fe^0 are located at 6.44, 7.09, 0.69 and 0.711 keV respectively. The microanalysis also confirms, the presence of a minimum quantity of oxygen; however the intensity is near the level of noise.

The magnetic properties of the Fe^0 particles were measured using vibrating sample magnetometer (VSM). Measurements of iron specific magnetization versus applied field are shown in Fig. 3. The magnetic properties of these particles can be described by the dependence of the magnetic induction (B) on the magnetic field (H). These particles exhibited ferromagnetism and monodominium behaviour because their presented a small coercivity. That means, when the ferromagnetic particles were removed from the field, they exhibited non-permanent magnetization. In this case, of particles of Fe^0 used in this work, had a coercivity value of 112.23 Oe, this represents a soft magnet while the saturation magnetization was 174.87 emu/g. This value is higher than values of

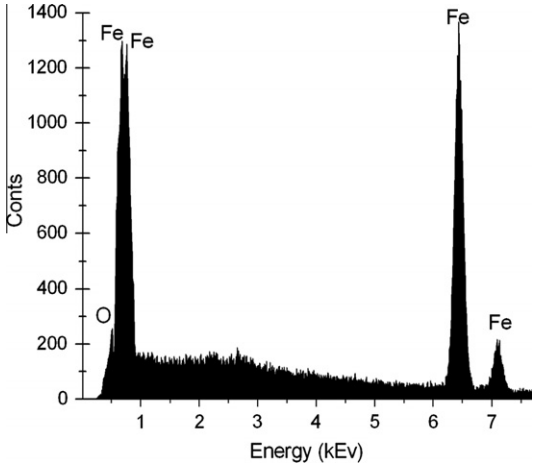

Fig. 2. EDX spectrum microanalysis of Fe^0 nanoparticles.

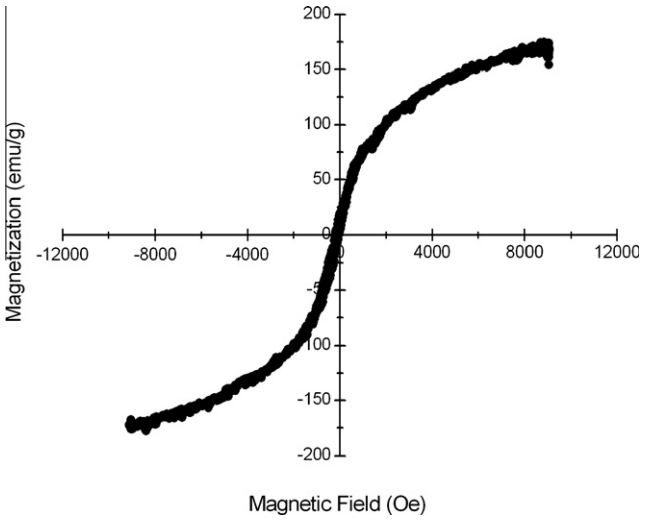

Fig. 3. Specific magnetization versus applied field curve of Fe^0 nanoparticles.

magnetization reported for magnetite particles [42,43], which indicates a superparamagnetic behaviour. How it is known, a material in a paramagnetic phase is characterized by randomly oriented (or uncoupled) magnetic dipoles, which can be aligned only in the presence of an external magnetic field and along its direction. This type of material has no coercivity nor remanence, as it was said, which means that when the external magnetic field is switched off, the internal magnetic dipoles randomize again, no extra energy is required to demagnetize the material and hence the initial zero net magnetic moment is spontaneously recovered [44,45].

Next effect of encapsulation of iron particles within polymethyl methacrylate was explored. The encapsulation process was made by means of emulsion polymerization techniques in a semicontinuous reactor. The iron particles were used as seed in the polymerization process. An emulsifier agent was used in order to disperse the iron particles in dispersed medium. Ionic and non-ionic emulsifiers were provided however the Rhodasurf L-4 a surfactant non-ionic from Rhodia yielded better dispersion results. Its concentration in the pre-emulsion was maintained below to CMC in order to prevent the formation of micelles. In the encapsulation process, the starved feed condition was established. Three different final average diameters of nanocomposites were produced. The concentration of polymethyl methacrylate was increased when the final diameter of nanocomposite was increased, and the concentration of particles was kept constant in the three systems. The final average diameters measured by DLS for the three samples were 98 nm, 128 nm and 161 nm.

Fig. 4 shows SEM images of the iron particles encapsulated by means of emulsion polymerization with polymethyl methacrylate for the three samples previously mentioned and the average diameter distribution as measured by DLS. The particles show a almost spherical morphologies and a high polydispersity indexes. It was not confirmed whether or not all of the nanocomposite particles in each system had the same concentration of Fe^0.

The specific magnetization as a function of applied magnetic field of the Fe^0 particles encapsulated within polymethyl methacrylate is reported in Fig. 5. For each of the three average diameter systems, the magnetization measurements were made using the same method as for the bare Fe^0 particles. The results indicate that the magnetic properties of nanocomposites particles are a function of the amount of polymer added. The saturation magnetization values for the nanocomposites with final average diameter of 98 nm, 128 nm and 161 nm, determined by dynamic light scattering were 127.25 emu/g, 69.99 emu/g and 48.56 emu/g respectively. From the results, the particles with an average diameter of 161 nm exhibited the lowest values of magnetization among the three encapsulated particle system and as compared to the bare Fe^0 particle.

In the three cases, at the same case of Fe^0 particles, the behaviour of material is considered as a superparamagnetic and a soft

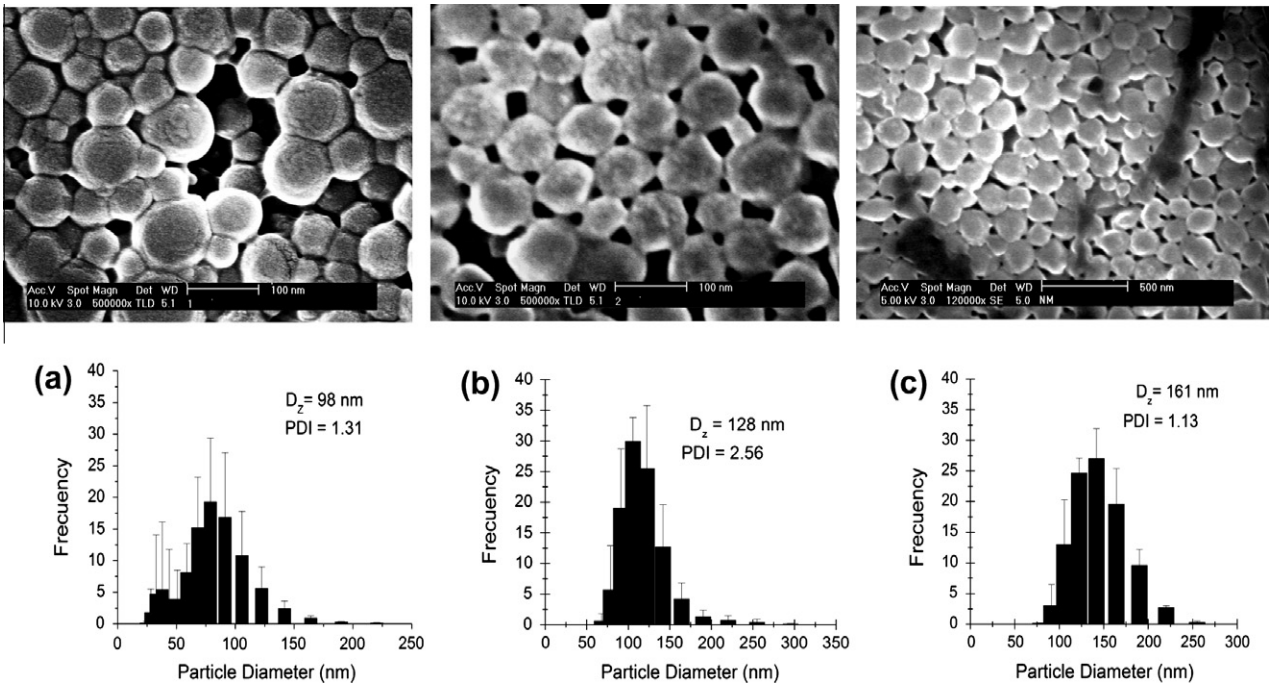

Fig. 4. SEM images of Fe^0 encapsulated within polymethyl methacrylate and the average diameter distribution of particle determined by DLS yielding average diameters of: (a) 98 nm, (b) 128 nm and (c) 161 nm.

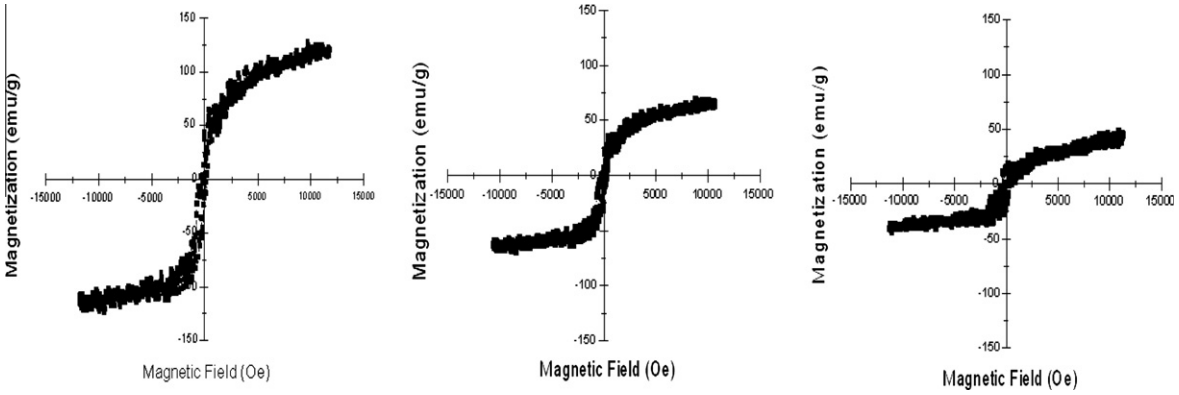

Fig. 5. Specific magnetization versus applied field curve of Fe^0 nanoparticles encapsulated within polymethyl methacrylate with an average diameter of: (a) 98 nm, (b) 128 nm and (c) 161 nm.

magnet because the values of coercivity were 168.77 Oe, 104.07 Oe and 171.22 Oe, respectively.

4. Conclusions

SEM images of bare Fe^0 particles show that they exhibited spherical morphologies, while EDX microanalysis revealed a signal corresponding to Fe^0 in addition to a low quantity of oxygen. SEM images of the Fe^0 particles encapsulated within polymethyl methacrylate show that the particles had almost spherical morphologies. The magnetization values of the Fe^0 nanoparticles were largest than those reported for magnetite. As the polymer concentration increased in the nanocomposites their magnetic properties were found to decrease.

Acknowledgment

To CONACyT by the financial support.

References

[1] D. Thassu, M. Deleers, Y. Pathak, Nanoparticulate Drug Delivery Systems, vol. 166, Drugs and the Pharmaceutical Sciences, New York, USA, 2007, p. 1.
[2] R. Richards, H. Bönnemann, Synthesis Approaches to Metallic Nanomaterials, in: C.S.S.R. Kumar, J. Hormes, C. Leuschner (Eds.), Nanofabrication towards Biomedical Applications: Techniques, Tools, Applications and Impact, WILEY-VCH, Federal Republic of Germany, 2005, p. 3.
[3] J. Zhou, J. Ralston, R. Sedev, D.A. Vétale, J. Colloid Interface Sci. 331 (2009) 251.
[4] K.D. Belfield, L. Zhang, Chem. Mater. 18 (2006) 5929.
[5] K. Vimala, K. Samba Sivudu, Y. Murali Mohan, B. Sreedhar, K. Mohana Raju, Carbohydr. Polym. 75 (2009) 463.
[6] I. Csetmeki, M. Kabai Faix, A. Szilágyi, A.L. Kovács, Z. Németh, M. Zringy, J. Polym. Sci., Part A: Polym. Chem. 42 (2004) 4802.
[7] A. Taden, M. Antonietti, A. Heilig, K. Landfester, Chem. Mater. 16 (2004) 5081.
[8] Z. Qian, Z. Zhang, Y. Chen, J. Colloid Interface Sci. 327 (2008) 354.
[9] A. Kumar Gupta, M. Gupta, Biomaterials 26 (2005) 3995.
[10] A. Elaissari, F. Sauzedde, F. Montage, C. Pichot, Preparation of magnetic latices, in: A. Elaissari (Eds.), Colloidal Polymers. Synthesis and Characterization, Surfactant Science Series, vol. 115, New York, 2003, p. 285.
[11] A.-Z. Chen, Y.-Q. Kang, X.-M. Pu, G.-F. Yin, Y. Li, J.-Y. Hu, J. Colloid Interface Sci. 330 (2009) 317.
[12] M. Hamoudeh, H. Fessi, J. Colloid Interface Sci. 300 (2006) 584.
[13] C. Ménager, O. Sandre, M. Jérôme, V. Cabuil, Polymer 45 (2004) 2475.
[14] S. Kiralp, A. Topcu, G. Bayramoğlu, M. Yakup Arica, L. Toppare, Sens. Actuators, B 128 (2008) 521.
[15] F. Sayar, G. Güven, E. Pişkin, J. Colloid Polym. Sci. 284 (2006) 965.
[16] S. Branconnot, C. Hoang, H. Fessi, A. Elaissari, Mater. Sci. Eng. C 29 (2009) 624.
[17] F. Montagne, O. Mondain-Monval, C. Pichot, A. Elaïsari, J. Polym. Sci., Part A: Polym. Chem. 44 (2006) 2642.
[18] S. Pal, S.C. Alocilja, Bisens. Bioelectron. 24 (2009) 1437.
[19] C.E. Mora-Huertas, H. Fessi, A. Elaissari, Int. J. Pharm. 385 (2010) 113.
[20] A. Khan, Mater. Lett. 62 (2008) 898.
[21] D. Nagao, M. Yokoyama, S. Saeki, Y. Kobayashi, M. Konno, J. Colloid Polym. Sci. 286 (2008) 959.
[22] A. Distch, P.E. Laibinis, D.I.C. Wang, T.A. Hatton, Langmuir 21 (2005) 6006.
[23] M. Lansalot, M. Sabor, A. Elaissari, C. Pichot, J. Colloid Polym. Sci. 283 (2005) 1267.
[24] M. Lattuada, T.A. Hatton, Langmuir 23 (2007) 2158.
[25] J.L. Zhang, R.S. Srivastava, R.D.K. Misra, Langmuir 23 (2007) 6342.
[26] M. Racuciu, D.E. Creanga, V. Badescu, A. Airinei, J. Optoelectron. Adv. Mater. 9 (2007) 1530.
[27] J. Zhou, J. Ralston, R. Sedev, D.A. Beattle, J. Colloid Interface Sci. 331 (2009) 251.
[28] S.P. Gubin, Y.A. Koksharov, Inorg. Mater. 38 (2002) 1085.
[29] C.M. Sorensen, in: K.J. Klabunde, Nanoscale Materials in Chemistry, John Wiley, 2001, p. 162.
[30] J.C. O'Connor, J. Tang, in: J. Zhang, J.S. Miller (Eds.), Nanostructured Magnetic Materials in Magnetism: Molecules to Materials III, Wiley-VCH, Weinheim, 2001, p. 1.
[31] W.A. der Heer, in: Z.L. Wang, Nanomagnetism, Characterisation of Nanophase Materials, Wiley-VCH, Weinheim, 2000, p. 289
[32] G. Schmid, Nanoparticles. From Theory to Application, Wiley-VCH, Weinheim, 2004, p. 221.
[33] D. Rosická, J. Sěmbera, Nanoscale Res Lett., 2010 (open access).
[34] E.E. Carpenter, J. Magn. Magn. Mater. 225 (2001) 17.
[35] J.L. Arias, F. Linares-Molinero, V. Gallardo, A.V. Delgado, J. Pharm. Sci. 33 (2008) 252.
[36] M.A. Abshinova, A.V. Lopatin, N.E. Kazantseva, J. Vilčàkovà, P. Sáha, Composites Part A 38 (2008) 2471.
[37] D.A. Perrin, Purification of Laboratory Chemicals, Pergamon Press, Oxford, 1966.
[38] R.A. Andersen, K. Faegri Jr., J.C. Green, A. Haaland, M.F. Lappert, W. Leung, K. Rypdal, Inorg. Chem. 27 (1988) 1782–1786.
[39] H. Xu, L. Cui, N. Tong, H. Gu, J. Am. Chem. Soc. 128 (2006) 15582.
[40] E.A. Collins, in: P.A. Lovel, M.S. El-Aasser (Eds.), Measurement of Particle Size and Particle Size Distribution in Emulsion Polymerization and Emulsion Polymers, John Wiley & Sons, England, 1997, p. 398.
[41] M. Nombra, M. Harada, W. Eguchi, S. Nagata, in: S.L. Piierma, J.L. Gardon (Eds.), Emulsion Polymerization, ACS Symp. Ser., Am. Chem. Soc., Washington, DC, 1976, p. 24 (Chapter 7).
[42] F. Yan, J. Zhang, F. Liu, W. Yang, J. Nanopart. Res. 11 (2009) 289.
[43] X. Liu, Y. Guan, Z. Ma, H. Liu, Langmuir 20 (2004) 10278.
[44] R.H. Kodama, J. Magn. Magn. Mater. 200 (1999) 359.
[45] A. Figuerolaa, R. Di Coratob, L. Mannaa, T. Pellegrino, Pharm. Res. 62 (2010) 126.